ISSN 0869-5911, Petrology, 2006, Vol. 14, No. 6, pp. 530–539. © Pleiades Publishing, Inc., 2006.
Original Russian Text © A.A. Borisov, 2006, published in Petrologiya, 2006, Vol. 14, No. 6, pp. 564–575.

Experimental Study of the Effect of SiO_2 on Ni Solubility in Silicate Melts

A. A. Borisov

Institute of Geology of Ore Deposits, Petrography, Mineralogy, and Geochemistry, Russian Academy of Sciences, Staromonetnyi per. 35, Moscow, 119017 Russia

E-mail: aborisov@igem.ru

Received November 9, 2005

Abstract—The solubility of Ni in silicate melts with variable SiO_2 content was studied at a total pressure of 1 atm within a wide range of temperature and oxygen fugacity. The maximum solubility of Ni (minimum activity coefficient of NiO) was observed in melts with ~55–57 wt % SiO_2, regardless of temperature and oxygen fugacity. Melts beyond this range showed significantly lower Ni solubility and, correspondingly, higher NiO activity coefficients. The analysis of our results and literature data led us to the conclusion that the NBO/T (number of nonbridging oxygen atoms per tetrahedrally coordinated atom) is inadequate to describe the effect of melt composition on Ni solubility.

DOI: 10.1134/S0869591106060026

INTRODUCTION

Magmatic melts show wide variations in SiO_2, from less than 44 wt % in ultrabasic rocks to more than 73 wt % in rhyolites (*Igneous rocks*, 1983). The effect of SiO_2 on the chemical properties of silicate melts (for example, activity coefficients of melt components) is therefore of special interest. As the first step, we studied the effect of SiO_2 on Ni solubility (activity coefficient of NiO) in silicate melts.

This study was additionally motivated by a desire to solve one contradiction. The effect of SiO_2 on Ni solubility in the melts of the pseudobinary system DA–SiO_2 (DA is the diopside–anorthite eutectic composition) was investigated at 1350°C by Ertel et al. (1997), who concluded that an increase in SiO_2 content in the melt from 50 to 60 wt % does not influence Ni solubility. O'Neill and Eggins (2002) confirmed this conclusion and showed that the solubility of Ni at 1400°C even decreases slightly in response to the addition of 50% quartz to the DA starting composition (Table 3 in O'Neill and Eggins, 2002). These results appeared to be surprising, because TiO_2, like SiO_2, is a network former, and an increase in its content in a melt enhances metal solubility (O'Neill and Eggins, 2002; Borisov et al., 2004).

EXPERIMENTAL METHODS

Experiments were conducted in a vertical tube furnace under controlled oxygen fugacity at the Institute of Geology and Mineralogy, University of Köln, Germany. Oxygen fugacity was controlled by a CO/CO_2 gas mixture; oxygen fugacity corresponding to a given gas ratio at a temperature of 1400°C was calculated using tables from Deines et al. (1974). Temperature in the working zone of the furnace was determined using a Pt–Rh thermocouple calibrated against the melting points of Au (1064°C) and Ni (1453°C). Experimental temperature and $\log f_{O_2}$ were estimated to be accurate within ±2°C and ±0.2, respectively.

The experiments were conducted using a loop technique, i.e., a melt droplet was suspended from a loop prepared from a narrow strip of Ni foil (0.125 mm thick and ~3 mm inner diameter) and saturated in Ni.

The starting mixtures were prepared from the eutectic anorthite–diopside composition (DA) by adding ~12, 25, 50, and 70% SiO_2 (compositions DA, DAS12, DAS25, DAS30, DAS50, and DAS70, respectively).

As the loop was dissolved, the melt at the contact was saturated in metal. Owing to diffusion and convection (Borisov, 2001) during the exposure, the Ni content was equalized over the melt droplet and equilibrated with that in the loop (with pure Ni, in our case), after which loop dissolution ceased and an increase in the Ni content of the melt stopped. After a necessary exposure at desired temperature and oxygen fugacity, the samples were quenched in the cold top zone of the furnace.

The main problem in experimental geochemistry and petrology is to prove the attainment of equilibrium between phases, in our case, between the metal and the melt. Special attention was paid to this problem in this study. The attainment of equilibrium was controlled by time series experiments and by approaching equilibrium from two sides (reversal experiments).

The quenched glasses were analyzed with a JEOL Superprobe microprobe at the Institute of Geology and Mineralogy, Köln University, Germany. Natural albite,

Table 1. Experimental conditions and compositions of experimental glasses (wt %)

Sample*	*T*, °C	CO_2/CO"	$-\log f_{O_2}$	Exp.+	SiO_2	s.d.	Al_2O_3	MgO	CaO	NiO	s.d.	Total	Phases#
DANi-95	1400	4.00	7.41	11.0	48.06	0.37	14.84	10.59	23.24	2.39	0.03	99.13	*L*
DAS50Ni-95	″	″	″	″	65.43	0.74	9.96	6.98	15.52	2.34	0.04	100.23	*L*
DAS50Ni-95R	″	″	″	″	65.54	0.31	9.88	6.95	15.41	2.54	0.03	100.32	*L*
DANi-93	1400	4.00	7.41	25.0	48.98	0.47	15.12	10.50	23.56	2.39	0.04	100.55	*L*
DAS50Ni-93	″	″	″	″	64.31	0.53	9.97	6.97	15.45	2.38	0.03	99.08	*L*
DAS50Ni-93R	″	″	″	″	65.36	0.23	9.96	6.95	15.50	2.49	0.03	100.25	*L*
DANi-94	1400	4.00	7.41	70.0	48.54	0.28	14.95	10.56	23.43	2.42	0.03	99.90	*L*
DAS12Ni-94	″	″	″	″	52.77	0.57	13.72	9.66	21.35	2.62	0.04	100.11	*L*
DAS25Ni-94	″	″	″	″	57.42	0.22	12.53	8.72	19.48	2.71	0.03	100.86	*L*
DAS50Ni-94	″	″	″	″	65.65	0.29	10.02	6.95	15.55	2.43	0.04	100.60	*L*
DAS50Ni-94R	″	″	″	″	65.69	0.50	10.00	6.92	15.57	2.46	0.03	100.65	*L*
DAS25Ni-101	1430	15.00	5.96	59.0	51.45	0.18	11.25	7.91	17.42	12.50	0.14	100.53	*L*
DAS30Ni-101	″	″	″	″	51.96	0.25	11.01	7.56	16.81	12.87	0.10	100.21	*L*
DAS50Ni-101	″	″	″	″	57.85	0.21	9.04	6.31	13.91	12.89	0.10	100.00	*L*
DAS70Ni-101	″	″	″	″	60.73	0.21	8.26	5.73	12.71	12.41	0.08	99.84	*L* + *Cr*
DANi-96	1430	4.00	7.10	59.0	49.05	0.23	15.08	10.57	23.38	2.81	0.05	100.89	*L*
DAS12Ni-96	″	″	″	″	52.92	0.31	13.76	9.61	21.27	3.06	0.04	100.62	*L*
DAS25Ni-96	″	″	″	″	56.61	0.36	12.44	8.73	19.26	3.18	0.05	100.22	*L*
DAS50Ni-96	″	″	″	″	54.69	0.74	9.94	6.89	15.29	2.95	0.05	99.76	*L*
DAS50Ni-96R	″	″	″	″	64.39	0.73	9.90	6.94	15.26	2.97	0.04	99.45	*L*
DANi-100	1430	0.25	9.51	69.5	50.42	0.15	15.44	10.68	24.16	0.187	0.003	100.89	*L*
DAS12Ni-100	″	″	″	″	54.68	0.11	14.05	9.78	22.06	0.201	0.005	100.77	*L*
DAS25Ni-100	″	″	″	″	58.40	0.41	13.02	8.89	20.20	0.201	0.005	100.71	*L*
DAS50Ni-100	″	″	″	″	66.58	0.15	10.31	7.10	16.01	0.172	0.006	100.17	*L*
DANi-99	1300	4.00	8.52	20.0	49.21	0.17	15.59	10.56	24.23	1.38	0.03	100.97	*L*
DAS25Ni-99	″	″	″	″	57.08	0.37	12.90	8.76	20.05	1.50	0.03	100.29	*L*
DAS25Ni-99R	″	″	″	″	57.18	0.42	12.89	8.76	19.98	1.56	0.02	100.36	*L*
DANi-98	1300	4.00	8.52	91.0	49.71	0.16	15.14	10.50	23.81	1.41	0.03	100.57	*L*
DAS12Ni-98	″	″	″	″	53.44	0.22	14.12	9.60	21.99	1.52	0.03	100.67	*L*
DAS25Ni-98	″	″	″	″	57.65	0.32	12.79	8.73	19.87	1.48	0.03	100.52	*L*
DAS25Ni-98R	″	″	″	″	57.65	0.21	12.80	8.71	19.86	1.50	0.02	100.53	*L*
DAS50Ni-98	″	″	″	″	62.86	0.38	11.16	7.50	17.17	1.35	0.04	100.05	*L* + *Cr*

Note: *R* designates the reverse experiment (approach to equilibrium from above). s.d. is standard deviation.
* Identical numbers for several samples mean that they were obtained during a single run.
" Proportions of gases in buffering mixtures.
+ Exposure in hours.
# Phase abbreviations: *L*, melt and *Cr*, cristobalite.

corundum, diopside, and metallic Ni were used as standards. The operating conditions were as follows: an accelerating voltage of 15 kV, a beam current of 15 nA, and a counting time of 40 s. The most reduced glasses (with Ni content at the ppm level) were measured at 500 nA and a counting time of up to 100 s. From 30 to 60 points were analyzed in each sample. Average compositions and experimental conditions are presented in Table 1.

RESULTS AND DISCUSSION

Time of the Attainment of Equilibrium in Silicic and Basic Melts

Figure 1 shows the results of experiments on determining the time required to attain equilibrium in silicic melts DAS50 (at 1400°C) and DAS25 (at 1300°C). Glasses for the reversal experiments were preliminarily melted under more oxidizing conditions and contained

Table 2. Activity coefficients of NiO and X_{NiO} and NBO/T values for melts obtained in long-duration experiments

Sample*	T, °C	$-\log f_{O_2}$	γ_{NiO}	s.d.	X_{SiO_2}	NBO/T
DANi-94	1400	–7.41	2.945	0.040	0.4848	1.027
DAS12Ni-94	″	″	2.723	0.043	0.5265	0.908
DAS25Ni-94	″	″	2.646	0.033	0.5693	0.794
DAS50Ni-94	″	″	2.945	0.046	0.6531	0.596
DAS50Ni-94R	″	″	2.909	0.040	0.6532	0.596
DAS25Ni-101	1430	–5.96	2.395	0.027	0.5219	1.047
DAS30Ni-101	″	″	2.313	0.017	0.5298	1.021
DAS50Ni-101	″	″	2.305	0.018	0.5912	0.857
DAS70Ni-101	″	″	2.391	0.015	0.6214	0.774
DANi-96	1430	–7.10	2.914	0.055	0.4856	1.023
DAS12Ni-96	″	″	2.661	0.031	0.5260	0.910
DAS25Ni-96	″	″	2.553	0.042	0.5653	0.810
DAS50Ni-96	″	″	2.730	0.049	0.6497	0.606
DAS50Ni-96R	″	″	2.713	0.039	0.6484	0.611
DANi-100	1430	–9.51	2.750	0.050	0.4969	0.958
DAS12Ni-100	″	″	2.555	0.064	0.5396	0.845
DAS25Ni-100	″	″	2.550	0.058	0.5774	0.743
DAS50Ni-100	″	″	2.963	0.102	0.6623	0.554
DANi-98	1300	–8.52	3.179	0.061	0.4925	0.988
DAS12Ni-98	″	″	2.955	0.066	0.5299	0.878
DAS25Ni-98	″	″	3.025	0.060	0.5726	0.769
DAS25Ni-98R	″	″	2.980	0.044	0.5726	0.768
DAS50Ni-98	″	″	3.289	0.088	0.6279	0.634

Note: *R* designates the reverse experiment (approach to equilibrium from above). s.d. is standard deviation.
* Identical numbers for several samples mean that they were obtained during a single run.

7–9 wt % NiO. As can be seen from Fig. 1, no less than 70 h was needed to attain equilibrium in silicic melt DAS50 (about 67 wt % SiO_2) at 1400°C. The more basic DA melt was found to be equilibrated at the same temperature within 4 h (Borisov, 2001). An estimate of 4 h could be too optimistic. However, as can be seen from Table 1, DA melt showed the same NiO content after 11-h and 70-h experiments (2.39 ± 0.03 and 2.42 ± 0.03 wt %, respectively).

It was anticipated that the DAS50 composition has to be saturated in cristobalite at 1300°C (Clark et al., 1962). Therefore, the DAS25 composition with 57 wt % SiO_2 was chosen to estimate the time of equilibration at this temperature. As can be seen in Fig. 1, this melt with a significantly lower SiO_2 content relative to DAS50 reached equilibrium from below within 20 h. It is noteworthy that the melt from the reverse experiment (attainment of equilibrium from a high Ni content) remained oversaturated in Ni relative to the equilibrium value after a 20-h exposure.

Why does a silicic melt require longer exposures to attain equilibrium than a basic melt? It is known that the loop–melt equilibrium is controlled by two processes: diffusion of the loop material (Ni, in the given case) in the melt and convection, which continuously homogenizes the melt during the experiment (Borisov, 2001). At the same time, the following statement holds for most elements: the higher the melt viscosity, the lower the diffusion coefficients of these elements in the given melt, all other conditions being equal (for example, Mungall, 2002). Thus, the high viscosity of silicic melts in combination with slower Ni diffusion results in longer exposures necessary to attain equilibrium.

In the following discussion, we will consider the results of the longest experiments. Although the melts with moderate SiO_2 contents attained equilibrium in shorter experiments, it is more plausible to consider the melt composition effect for samples obtained in a single melting run, i.e., at absolutely identical T–f_{O_2} parameters. The structural–chemical and thermodynamic characteristics (NBO/T, $\log\gamma_{NiO}$ and others) of the discussed melts are shown in Table 2.

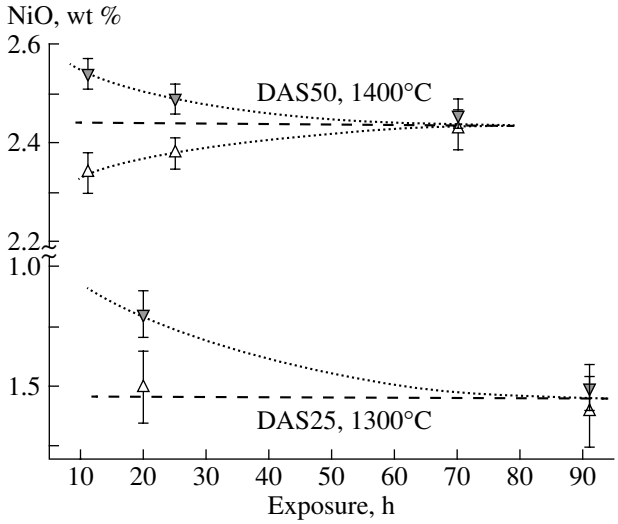

Fig. 1. Time necessary for the attainment of equilibrium in silicic melts DAS50 (at 1400°C) and DAS25 (at 1300°C). Open symbols are direct experiments (starting compositions are Ni-free), and filled symbols are reverse experiments (starting NiO content is higher than equilibrium one).

Effect of Oxygen Fugacity and Temperature on Ni Solubility

The solubility of Ni in the melts can be described by the reaction

$$\text{Ni (metal)} + 0.5O_2 = \text{NiO (silicate melt)}. \quad (1)$$

The theoretical slope (k) of the logarithm of Ni solubility versus $\log f_{O_2}$ at a fixed temperature is 1/2.

The solubility of Ni as a function of f_{O_2} at a fixed temperature of 1430°C is shown in Fig. 2. All points regardless of melt composition define a single linear trend corresponding to the equation:

$$\log(\text{NiO, wt \%}) = 0.51 \log f_{O_2} + 4.123. \quad (2)$$

The fact that the value of k in Eq. (2) is close to the theoretical value of 1/2, as well as the very high correlation coefficient (R^2 = 0.999), testifies that oxygen fugacity is the main control on Ni solubility.

To calculate the temperature dependency of Ni solubility in silicate melts, we used three experimental series conducted under similar proportions of gases in the buffer mixture ($CO_2/CO = 4$), i.e., at relatively similar oxygen fugacity values. The data were recalculated to $f_{O_2} = 10^{-8}$ atm, assuming k = 1/2 (ideal value). Then the slope of $\log(\text{NiO, wt \%})$ versus $1/T(\text{K})$ (h) was calculated as 8465 ± 4, 8350 ± 45, 7828 ± 79, and 6653 ± 274 for the DA, DAS12, DAS25, and DAS50 compositions, respectively. It is seen that the temperature dependence tends to decrease for more silicic melts, although the slope h remains the same within the error. Additional studies of the temperature dependence of metal solubility in silicic melts are needed.

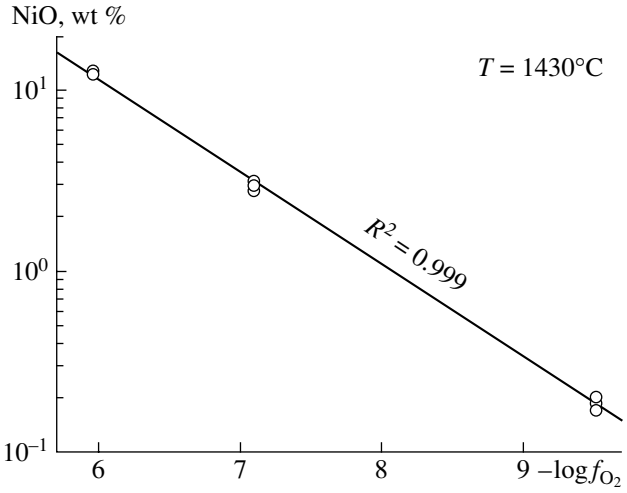

Fig. 2. Effect of oxygen fugacity on Ni solubility at a temperature of 1430°C.

Effect of SiO_2 on Ni Solubility in Silicate Melts. A Comparison with Literature Data

Figure 3 shows the results of three long-duration experimental series performed at identical gas proportions in the buffer mixture ($CO_2/CO = 4$), which implies a relatively constant oxygen fugacity (approximately an order of magnitude lower than that of the quartz–fayalite–magnetite buffer). It can be seen that the maximum Ni solubility in silicate melts is reached at intermediate SiO_2 contents (~55–58 wt %).

As was mentioned above, the experiments of Ertel et al. (1997) and O'Neill and Eggins (2002) were conducted in the same system (DA + SiO_2) at temperatures

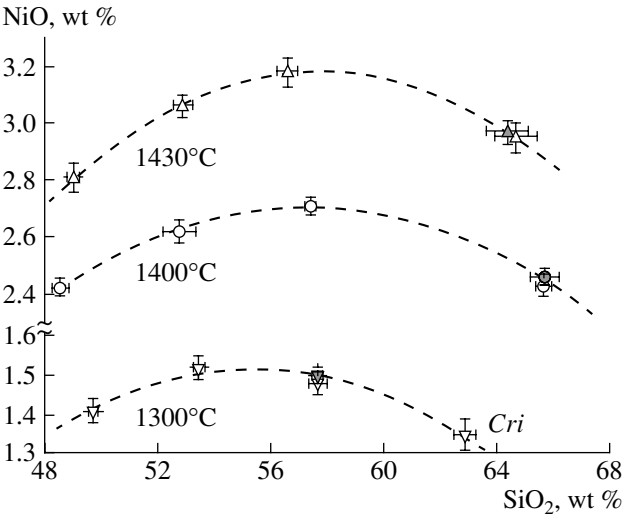

Fig. 3. Effect of SiO_2 content on Ni solubility in the melts of three experimental series at a constant relative oxygen fugacity (QFM – 1). *Cri* is the cristobalite-saturated composition. Open symbols are direct experiments, and filled symbols are reverse experiments.

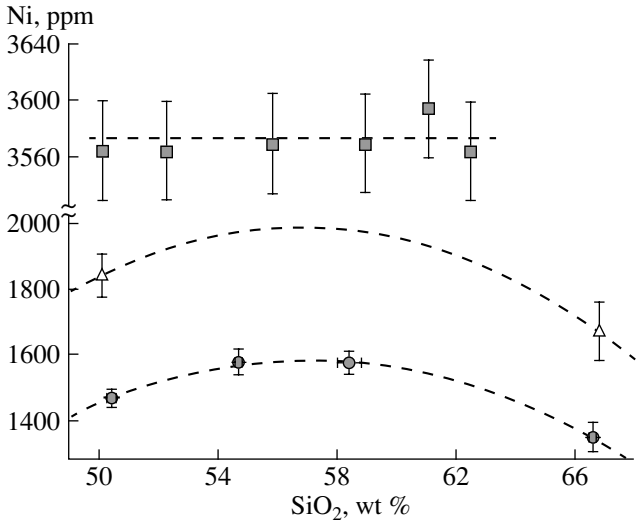

Fig. 4. Effect of SiO_2 content on Ni solubility in the melts of experimental series conducted at 1430°C and $f_{O_2} = 10^{-9.51}$ atm (filled circles). Also shown are data on Ni solubility in the melts of the same composition from the literature: at 1350°C and $f_{O_2} = 10^{-9.15}$ atm (Ertel et al., 1997; filled boxes); at 1400°C and $f_{O_2} = 10^{-9.60}$ atm (O'Neill and Eggins, 2002; open triangles).

of 1350 and 1400°C, respectively, and showed no SiO_2 effect on Ni solubility. Our experiments revealed a maximum in Ni solubility within a temperature interval from 1300 to 1430°C (Fig. 3). This discrepancy could be due to the low Ni content (on the ppm level) in the experiments of Ertel et al. (1997) and O'Neill and Eggins (2002). Therefore, one of our experimental series was conducted at low f_{O_2} to provide a ppm-level Ni solubility. Our results and the data of the cited authors are shown in Fig. 4. Our data for low Ni contents in melts agree with the results of experiments with percent-level Ni solubilities (compare with Fig. 3). Similar to the previous experimental series, the maximum Ni solubility is observed in melts with about 57 wt % SiO_2. As follows from Fig. 4, the data of O'Neill and Eggins (2002) are consistent with the possible existence of a maximum on the Ni solubility curve in melts with SiO_2 = 55–57 wt %, which were not investigated by these authors. In contrast, Ertel et al. (1997) carried out a series of experiments by adding quartz to the initial DA melt. Since they concluded that SiO_2 has no effect on Ni solubility in melt, we examine their results in more detail.

The experiments of Ertel et al. (1997) were conducted using a Ni crucible and a rotating pestle, which mixed the melt and promoted the rapid attainment of equilibrium (Dingwell et al., 1994). Since the melt volume was large (~2 g), the experiments lasted for hundreds of hours. The experimental design allowed sampling of melt aliquots for analysis and addition of a new portion of materials (in their experiments, quartz was added to the initial DA melt). These researchers believed that equilibrium was not attained either at the initial stage (starting DA composition) or during the first two additions of quartz (4.5 and 13%) (Ertel et al., 1997; p. 4715 and Fig. 2). The equilibrium Ni content was calculated by extrapolating the disequilibrium values using an equation proposed by Ertel et al. (1996). In our opinion, the data obtained in such a way can provide only rough estimates, and the extrapolation errors must be included into the total uncertainty, which was not done. According to Ertel et al. (1997), the equilibrium was attained during the subsequent stages of the experiment (addition of 21.5, 28.2, and 33% quartz). As was shown above, the equilibrium in silicic melts is attained slower than in basic melts. Thus, there is a reasonable question: if equilibrium was not attained in 238 h after quartz addition (Ertel et al., 1997; Table 2), how could it be attained during the subsequent stages with comparable exposure times? As follows from these considerations, the absence of correlation between Ni solubility and SiO_2 content in the experiments of Ertel et al. (1997) can be attributed to the absence of equilibrium and high extrapolation errors.

Effect of SiO_2 Content on the Activity Coefficients of NiO in Silicate Melts. A Comparison of X_{SiO_2} and NBO/T Structural Parameters

As follows from reaction (1), the activity coefficients of NiO in the melts can be calculated by the following way:

$$K_1 = a_{NiO}/(a_{Ni} f_{O_2}^{0.5}) = (X_{NiO}\gamma_{NiO})/f_{O_2}^{0.5}, \quad (3)$$

$$\gamma_{NiO} = (K_1 f_{O_2}^{0.5})/X_{NiO}, \quad (4)$$

where X_{NiO}, a_{NiO}, and γ_{NiO} are, respectively, the mole fraction, activity, and activity coefficient of NiO in the melt; K_1 is the constant of reaction (1); and $a_{Ni} = 1$ for pure metal. The calculated activity coefficients of NiO are listed in Table 2. The calculations were performed relative to a standard state of pure liquid NiO (Holzheid et al., 1997; O'Neill and Eggins, 2002).

One of the most widely used parameters characterizing the degree of melt polymerization is NBO/T (number of nonbridging oxygen atoms per tetrahedrally coordinated cation), which has been widely popularized in the geological literature by B. Mysen (e.g., Mysen, 1988). In such a case, all the components of melt are subdivided into network formers (SiO_2, TiO_2, Al_2O_3, and others) and network modifiers (Na_2O, CaO, FeO, and others). The calculation of this parameter implies that all network formers (for example, SiO_2 and Al_2O_3) equally contribute to the polymerization of melt, and all modifiers (for example CaO and FeO) have the same effect on melt depolymerization. This is

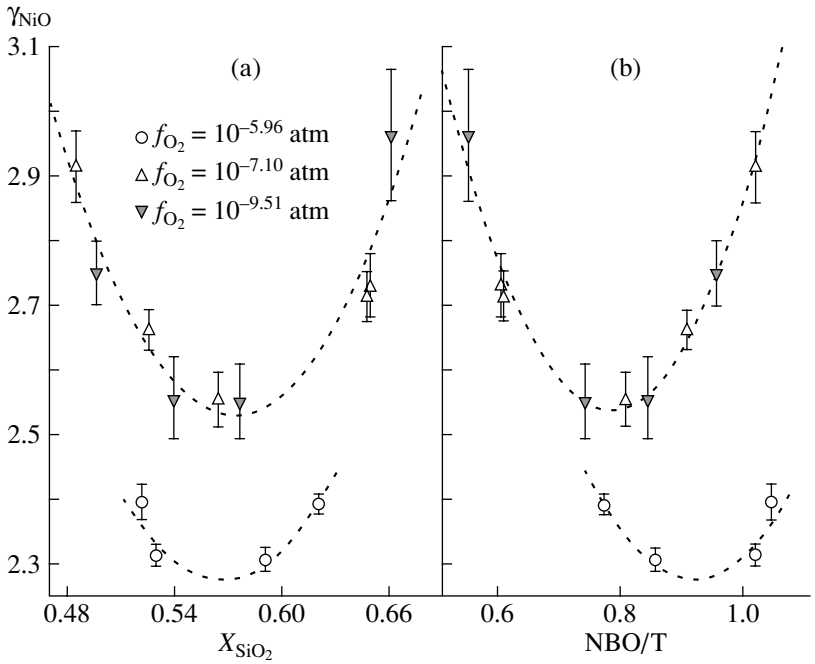

Fig. 5. Effect of (a) X_{SiO_2} and (b) NBO/T on γ_{NiO} in silicate melts of the DAS system at 1430°C.

obviously not the case. For instance, the constants of polymerization in the binary systems MO–SiO_2 vary considerably depending on the identity of M (Table 1 in Ottonello et al., 2001). The different behavior of cations in natural multicomponent melts is also supported by indirect evidence. For example, the empirical equations relating the proportions of ferrous and ferric Fe in silicate melts with intensive and extensive parameters (e.g., Sack et al., 1980) include the $\Sigma d_i X_i$ terms allowing for the effect of melt composition where X_i is the mole fraction of a major component, and d_i is the respective empirical coefficient. The sharp differences between the values of d_{CaO} and d_{FeO}, on the one hand, and d_{SiO_2} and $d_{Al_2O_3}$, on the other hand, indicate chemical and, correspondingly, structural nonequivalence of both network-forming and network-modifying oxides. However, NBO/T is widely used in empirical equations as a parameter describing the effect of melt composition (e.g., Righter et al., 1997). The values of NBO/T for our experimental melts are given in Table 2.

Figure 5 shows γ_{NiO} values for three experimental series conducted at a fixed temperature of 1430°C and oxygen fugacities of $10^{-5.96}$, $10^{-7.10}$, and $10^{-9.51}$ atm. The values of γ_{NiO} obtained in two reducing series can be approximated by a single curve, whereas the oxidizing series yielded somewhat different activity coefficient values. It is possible that Henry's law is not obeyed at very high NiO contents (12–13 wt % NiO).

It is interesting to compare the effect of X_{SiO_2} and NBO/T on the activity coefficient of NiO. In the former case (Fig. 5a), both curves display a minimum at approximately the same values of $X_{SiO_2} \approx 0.55$–0.57, whereas in the latter case (Fig. 5b), the minimum for the high-Ni melts is shifted towards higher NBO/T values relative to the low-Ni melts.

Pretorius and Muan (1992) also reported a distinct minimum of γ_{NiO} associating with regular variations in melt composition. They studied the behavior of Ni in the melts of the CaO–MgO–Al_2O_3–SiO_2 system (designated as CMNAS by these authors, and CMAS in the generally accepted abbreviation). In contrast to our experiments with the dilution of the DA composition by the addition of SiO_2, these authors performed experiments at a variable CaO/SiO_2 ratio and nearly constant MgO (about 6 wt %) and Al_2O_3 concentrations (~10 or ~20 wt %). In order to compare with our results, the data of Pretorius and Muan (1992) on Ni solubility were recalculated to the activity coefficients of NiO using the accepted here thermodynamic data and standard states. Figure 6 shows the calculated values of γ_{NiO} as a function of (a) X_{SiO_2} and (b) NBO/T. Like in Fig. 5, both curves (for $X_{Al_2O_3}$ of about 0.06 and 0.12) in Fig. 6a exhibit minima at $X_{SiO_2} \approx 0.55$–0.56, whereas in the γ_{NiO}–NBO/T diagram (Fig. 6b), the minimum for the high-Al melts is shifted towards higher NBO/T relative to the minimum for the low-Al melts.

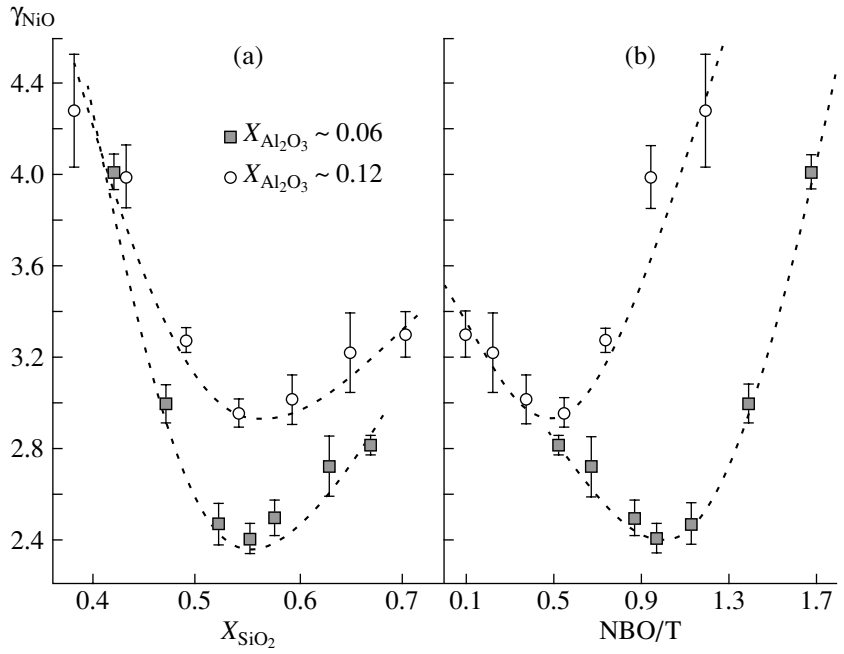

Fig. 6. Effect of (a) X_{SiO_2} and (b) NBO/T on γ_{NiO} in silicate melts of the CMAS system at 1400°C (Pretorius and Muan, 1992).

Extremes in Ni Solubility (γ_{NiO}) Curves: Possible Explanation

The values of γ_{NiO} from Table 2 were approximated at each temperature (high-Ni melts at 1430°C were considered separately) by the function of X_{SiO_2} (X):

$$\log \gamma_{NiO} = aX^2 + bX + c, \quad (5)$$

where a, b, and c are the empirical coefficients. The correlation coefficient varies from 0.80 to 0.99, indicating the plausibility of the chosen equation. The calculated curves are shown in Fig. 7. The temperature effect on the activity coefficient of NiO in the melt is evident: γ_{NiO} increases with decreasing temperature regardless of melt composition. However, we will further discuss the position of minima in the curves rather than the absolute values of γ_{NiO}.

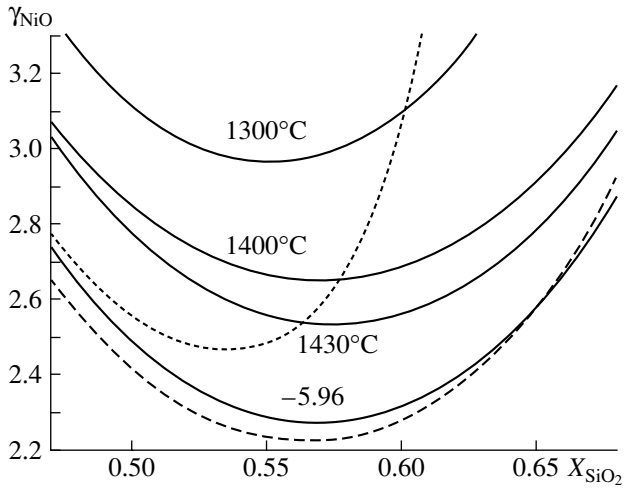

Fig. 7. Effect of X_{SiO_2} on γ_{NiO} in silicate melts: a comparison of experimental (solid line) and calculated (dashed and dotted lines) curves. Experimental data were approximated by Eq. (5). Numbers near the curves show temperature. The curve labeled –5.96 describes Ni-rich melts obtained in the most oxidizing conditions ($10^{-5.96}$ atm.). The dashed line is the model of subregular solid solutions (O'Neill and Eggins, 2002), and the dotted line is the model of Colson et al. (2005). See text for explanation.

It is interesting that three (at 1400 and 1430°C) from the four curves in Fig. 7 show a minimum at X_{SiO_2} = 0.571 ± 0.003, and it is shifted to X_{SiO_2} = 0.552 only at a temperature of 1300°C. It is possible that the minimum is really shifted toward more basic composition with decreasing temperature. However, the positions of minima on these curves must be considered as approximate estimates, because most of the curves were calculated using 4–5 points. Figure 6a (Pretorius and Muan, 1992; 1400°C) also supports that, independent of temperature and melt composition, the minimum of γ_{NiO} (maximum of Ni solubility at given T–f_{O_2} parameters) corresponds to melts with X_{SiO_2} = 0.55–0.57.

The existence of minima in the γ_{NiO} curves may be formally explained by applying the formalism of

subregular solid solutions (e.g., O'Neill and Eggins, 2002):

$$\log\gamma_{NiO} = \sum_{j=1}^{n}\sum_{k=1}^{j} a_{jk}X_jX_k. \quad (6)$$

The four-component CMAS system studied by them can be described by ten a_{jk} parameters. Although these authors expressed some doubt about the use of the ten-parameter equation obtained by processing 18 different compositions, we examined the applicability of this model for the description of the minimum in the γ_{NiO} curve [a_{jk} values were taken from Table 9 of O'Neill and Eggins (2002)]. Since these authors calculated the mole fractions of major components on a single-cation basis ($AlO_{1.5}$ instead of Al_2O_3), the obtained γ_{NiO} and X_{SiO_2} values were recalculated in accordance with those accepted in this paper. It appeared that Eq. (6) adequately reproduces the minimum in the γ_{NiO}–X_{SiO_2} coordinates. At 1400°C, the temperature at which Eq. (6) was calibrated, the value of γ_{NiO} is 2.43 in the starting DA system, decreases monotonously with increasing SiO_2 content in the melt, reaches a minimum (γ_{Ni} = 2.22) at X_{SiO_2} = 0.565, and returns to a starting value of 2.43 at X_{SiO_2} = 0.631. Both the X_{SiO_2} coordinate of the minimum and the shape of the model curve are similar to our experimental curves: on average, γ_{NiO} increases by 20% in response to a 10% increase or decrease in SiO_2 mole fraction in the melt relative to the minimum.

The extremes in the solubility (activity coefficient) curves can be explained by a less formal way by considering reaction (1) in combination with the following dissociation reaction of NiO dissolved in melt:

$$Ni^{2+}\ (melt) + O^{2-}\ (melt) = NiO\ (melt), \quad (7)$$

$$a_{NiO} = \gamma_{NiO}X_{NiO} = (a_{Ni^{2+}})(a_{O^{2-}})K_7. \quad (8)$$

Under given T–f_{O_2} parameters, a_{NiO} (or corresponding γ_{NiO} value) is then a function of two more or less independent parameters, $a_{Ni^{2+}}$ and $a_{O^{2-}}$.

In the simplest case, the value of $a_{Ni^{2+}}$ can be found, according to the Temkin (1946) model, as the fraction of Ni^{2+} in the sublattice of cation modifiers, $X_{Ni^{2+}}/(X_{Ca^{2+}} + X_{Mg^{2+}} + X_{NiO})$. Assuming that the fraction of undissociated oxides in the melt is low, this parameter can be approximated by $X_{NiO}/(X_{CaO} + X_{MgO})$, if the solubility of Ni is low. Then, Eq. (8) can be recast as

$$\gamma_{NiO} = (X_{CaO} + X_{MgO})^{-1}(a_{O^{2-}})K_7. \quad (9)$$

In more complex models, part of Al ions can be considered as modifiers, and different reaction ability of CaO and MgO can be taken into account using empirical correction factors for the molar fractions of these oxides (Colson et al., 2005).

The value of $a_{O^{2-}}$ can be estimated using the model of Toop and Samis (1962):

$$2O^- = O^0 + O^{2-}, \quad (10)$$

where O^-, O^0, and O^{2-} are nonbridging, bridging, and free oxygen ions, respectively.

For binary systems, the contents of various oxygen forms are defined by the amount of SiO_2 moles (N_{SiO_2}) as follows:

$$(O^0) = 2N_{SiO_2} - (O^-)/2, \quad (11)$$

$$(O^{2-}) = (1 - N_{SiO_2}) - (O^-)/2, \quad (12)$$

$$(O^-)^2(4K_{10} - 1) + (O^-)(2 + 2N_{SiO_2}) + 8N_{SiO_2}(N_{SiO_2} - 1) = 0, \quad (13)$$

where K_{10} is the constant of reaction (10).

The number of moles of all oxygen forms can be obtained by solving the system of Eqs. (11)–(13). It can be shown that the content of O^{2-} (and, correspondingly, $a_{O^{2-}}$) decreases monotonously with increasing SiO_2, and $(X_{CaO} + X_{MgO})^{-1}$ increases concurrently. The opposite variations of two factors in Eq. (9) must produce extremes in the curves of γ_{NiO} (or Ni solubility in melt) versus X_{SiO_2}. In the case of multicomponent melts, the calculation of the contents of O^{2-} and other structural units is more complicated (Ottonello et al., 2001). According to Colson et al. (2005), $a_{O^{2-}}$ has to be proportional to NBO^2/BO to a first approximation, where NBO and BO are the concentrations of nonbridging and bridging oxygen atoms, respectively.

The model of Colson et al. (2005) is not completely adequate, because it suggests the independence of NiO activity coefficients on temperature (model was calibrated using electrochemical measurements within a wide temperature range) and is valid for compositions with $0.3 < (X_{MgO} + X_{CaO}) < 0.55$. Nonetheless, Colson et al (2005) argued that their model is superior to the model of O'Neill and Eggins (2002), because it involves only five empirical coefficients (instead of 10).

According to the model of Colson et al. (2005), the addition of SiO_2 to the starting DA composition also results in the appearance of a γ_{NiO} minimum. However, neither the X_{SiO_2} coordinate of the minimum (0.535) nor the shape of the curve (10% increase in SiO_2 con-

tent relative to the minimum leads to an increase in γ_{NiO} by a factor of 2.3) agree with our experimental data.

Petrological Consequences

This paper considers a rather narrow range of silicate melt compositions. Nevertheless, our experiments may have some petrological applications on the behavior of Ni (and other elements) in silicate melts of the basalt–rhyolite series.

First, the maximum Ni solubility at $SiO_2 \sim 55$–58 wt % indicates that there are fundamental chemical differences between basic and silicic melts. Therefore, simple empirical relations (for example, the approximation of melt composition effects by the expressions $\Sigma d_i X_i$, where X_i is the mole fraction of a major component, and d_i is the empirical coefficient) obtained for a certain group of melts should be applied to other melts with caution. The $\Sigma d_i X_i$ term could be of limited application for the description of the effect of composition not only for activity coefficients (metal solubility) but also for the proportions of cations of different valence sates in silicate melts. For example, Nikolaev et al. (1996) showed that none of the existing empirical equations describing the Fe^{3+}/Fe^{2+} ratio in natural melts as a function of temperature, oxygen fugacity, and melt composition (all these equations include terms of the $\Sigma d_i X_i$ type) and calibrated using a basalt-dominated data base is adequate for silicic melts.

Second, it is not a mere coincidence that the minima of curves in the γ_{NiO}–X_{SiO_2} coordinates are observed at approximately the same SiO_2 contents (X_{SiO_2} = 0.55–0.57, Figs. 5a and 6a) independent of melt composition but are shifted in the γ_{NiO}–NBO/T diagram along the NBO/T axis depending on the concentrations of Ni and Al (Figs. 5a, 6b). This suggests that SiO_2 controls the chemistry and structure of silicate melts. Aluminum oxide is presumably a less efficient network former compared to SiO_2, and NiO is inferior to CaO and MgO as a network modifier.

In this regard, it is implausible to use NBO/T for the description of the effect of melt composition on various partition coefficients. In particular, Righter et al. (1997) used NBO/T to describe the effect of melt composition on the partition coefficients of Ni and other siderophile elements between metal and silicate melt. Since the value of D_{Ni} is inversely proportional to Ni solubility (and proportional to γ_{NiO}), all relations in the behavior of γ_{NiO} found in our study are applicable to D_{Ni}. As can be seen in Fig. 6b, variations in NBO/T between 0.5 and 1.0 exert opposite effects on γ_{NiO} in high-Al and low-Al melts, indicating an equivocal influence of NBO/T on D_{Ni} in melts of different compositions.

The most productive in this respect is the approach of Beattie et al. (1991), who calculated $D_i^{Ol/L}$ and $D_i^{Opx/L}$ (partition coefficients of Ca, Sc, Mn, Fe, Co, Ni, and Yb between olivine, orthopyroxene, and silicate melt) as functions of D_{Mg}. It is evidently that, if the activity coefficient of oxide i and γ_{MgO} depend on melt composition in a similar way, the linear dependence of D_i on D_{Mg} will hold for both silicic and basic melts. It should be noted that the general similarity of melt composition effects on the activity coefficients of many oxides was demonstrated by O'Neill and Eggins (2002) and Borisov et al. (2004).

CONCLUSIONS

Ni solubility in silicate melts with variable SiO_2 content was experimentally studied at a total pressure of 1 atm and temperatures of 1300–1430°C within an oxygen fugacity range providing NiO concentration in melts from a few ppm to 13 wt %.

It was shown that the Ni solubility shows a maximum (minimum activity coefficient of NiO) in melts with SiO_2 contents of about 55–57 wt %, independent of temperature and oxygen fugacity. The solubility of Ni is significantly lower (and, correspondingly, NiO activity coefficient is higher) in melts with both higher and lower SiO_2 contents.

Regardless of melt composition, γ_{NiO} increases with decreasing temperature between 1430 and 1300°C.

Based on our results and literature data, we concluded that the NBO/T parameter is the least suitable for the description of the effect of melt composition on Ni solubility.

ACKNOWLEDGMENTS

The author is grateful to A.A. Ariskin (Vernadsky Institute of Geochemistry and Analytical Chemistry, Russian Academy of Sciences) for the discussion of the structure of silicate melts, which led to a significant improvement of the manuscript. This study was supported by the German Science Foundation (DFG), Russian Foundation for Basic Research (project no. 05-05-64175), Program for Fundamental Research of the Earth Science Division, Russian Academy of Sciences, and the Federal Program for the Support of Leading Scientific Schools.

REFERENCES

1. E. D. Andreeva, V. A. Baskina, O. A. Bogatikov, et al., *Igneous Rocks: Classification, Nomenclature, and Petrography* (Nauka, Moscow, 1983) [in Russian].
2. P. Beattie, C. Ford, and D. Russel, "Partition Coefficients for Olivine–Melt and Orthopyroxene–Melt Systems," Contrib. Mineral. Petrol. **109**, 212–224 (1991).
3. A. Borisov, "Loop Technique: Dynamics of Metal/Melt Equilibration," Mineral. Petrol. **71**, 87–94 (2001).
4. A. Borisov, Y. Lahaye, and H. Palme, "The Effect of TiO_2 on Pd, Ni and Fe Solubilities in Silicate Melts," Am. Mineral. **89**, 564–571 (2004).

5. S. P. Clark, J. F. Schairer, Jr., and J. De Neufville, "Phase Relations in the System $CaMgSi_2O_6$–$CaAl_2SiO_6$–SiO_2 at Low and High Pressure," Carnegie Inst. Washington, Year Book **61**, 59–68 (1962).
6. R. O. Colson, A. M. Floden, T. R. Haugen, et al., "Activities of NiO, FeO, and O^{2-} in Silicate Melts," Geochim. Cosmochim. Acta **69**, 3061–3073 (2005).
7. P. S. Deines, R. H. Nafziger, G. C. Ulmer, and E. Woermann, "Temperature–Oxygen Fugacity Tables for Selected Gas Mixtures in the System C–H–O at One Atmosphere Total Pressure," Bull. Earth Miner. Sci., Exp. St. **88** (1974).
8. D. B. Dingwell, H. St. C. O'Neill, W. Ertel, and B. Spettel, "The Solubility and Oxidation State of Ni in Silicate Melts at Low Oxygen Fugacities: Results Using a Mechanically Assisted Equilibration Technique," Geochim. Cosmochim. Acta **58**, 1967–1974 (1994).
9. W. Ertel, D. B. Dingwell, and H. St. C. O'Neill, "Solubility of Tungsten in a Haplobasaltic Melt as Function of Temperature and Oxygen Fugacity," Geochim. Cosmochim. Acta **60**, 1171–1180 (1996).
10. W. Ertel, D. B. Dingwell, and H. St. C. O'Neill, "Compositional Dependence of the Activity of Nickel in Silicate Melts," Geochim. Cosmochim. Acta **61**, 4707–4721 (1997).
11. A. Holzheid, H. Palme, and S. Chakraborty, "The Activities of NiO, CoO and FeO in Silicate Melts," Chem. Geol. **139**, 21–38 (1997).
12. J. E. Mungall, "Empirical Models Relating Viscosity and Tracer Diffusion in Magmatic Silicate Melts," Geochim. Cosmochim. Acta **66**, 125–143 (2002).
13. B. O. Mysen, *Structure and Properties of Silicate Melts* (Elsevier, Amsterdam, 1988).
14. G. S. Nikolaev, A. A. Borisov, and A. A. Ariskin, "Calculation of the Ferric–Ferrous Ratio in Magmatic Melts: Testing and Additional Calibration of Empirical Equations for Various Magmatic Series," Geokhimiya, No. 8, 713–722 (1996) [Geochem. Int. **34**, 641–649 (1996)].
15. H. St. C. O'Neill and S. M. Eggins, "The Effect of Melt Composition on Trace Element Partitioning: An Experimental Investigation of the Activity Coefficients of FeO, NiO, CoO, MoO_2 and MoO_3 in Silicate Melts," Chem. Geol. **186**, 151–181 (2002).
16. G. Ottonello, R. Moretti, L. Marini, and M. V. Zuccolini, "Oxidation State of Iron in Silicate Glasses and Melts: A Thermochemical Model," Chem. Geol. **174**, 157–179 (2001).
17. E. B. Pretorius and A. Muan, "Activity of Nickel (II) Oxide in Silicate Melts," J. Am. Ceram. Soc. **75**, 1490–1496 (1992).
18. K. Righter, M. J. Drake, and G. Yaxley, "Prediction of Siderophile Element Metal–Silicate Partitioning Coefficients to 20 GPa and 2800°C: the Effect of Pressure, Temperature, Oxygen Fugacity, and Silicate and Metallic Melt Compositions," Phys. Earth Planet. Inter. **100**, 115–134 (1997).
19. R. O. Sack, I. S. E. Carmichael, M. Rivers, and N. S. Ghiorso, "Ferric–Ferrous Equilibria in Natural Silicate Liquids at 1 bar," Contrib. Mineral. Petrol. **75**, 369–376 (1980).
20. M. Temkin, "Mixtures of Molten Salts as Ionic Solutions," Zh. Fiz. Khim. **20** (1), 105–110 (1946).
21. G. W. Toop and C. S. Samis, "Activities of Ions in Silicate Melts," Trans. Metall. Soc. AIME **224**, 878–887 (1962).